JACC Vol. 31, No. 7
June 1998:1547–54

Intravenous Electron-Beam Computed Tomographic Coronary Angiography for Segmental Analysis of Coronary Artery Stenoses

AXEL SCHMERMUND, MD,* BENNO J. RENSING, MD, PHD,† PATRICK F. SHEEDY, MD, MALCOLM R. BELL, MBBS, FRACP, JOHN A. RUMBERGER, MD, PHD, FACC

Rochester, Minnesota and Rotterdam, The Netherlands

Objectives. **We sought to identify and localize significant coronary stenoses on a segmental basis by electron-beam computed tomography (EBCT) and intravenous administration of a contrast agent.**

Background. **The clinical applicability and limitations of intravenous EBCT coronary angiography have not been defined.**

Methods. **EBCT was performed within 24 h of selective coronary angiography (SCA) in 28 patients (19 men and 9 women, mean [±SD] age 60 ± 10 years). After examination for coronary calcium, EBCT coronary angiography was performed using overlapping slices (in-plane resolution 0.34 to 0.41 mm) with a nominal slice thickness of 1 mm. Based on quantitative analysis of SCA, lumen diameter narrowing ≥50% (i.e., significant stenoses) was evaluated in 8 (major) or 12 (including side branches) coronary artery segments, using both two-dimensional (tomographic) and three-dimensional (volume) data sets.**

Results. **Of the 330 segments assessable by SCA, 237 (72%) were visualized by EBCT. The sensitivity (±SE) for detection of significant stenoses was 82 ± 6%; specificity was 88 ± 2%; positive and negative predictive values were 57 ± 7% and 96 ± 2%, respectively; and overall accuracy was 87 ± 2%. If only eight (major) coronary artery segments were considered, 194 (88%) of 221 segments were visualized, and the overall accuracy was 90 ± 2%. Seven (18%) of 38 significantly stenotic segments were classified as having <50% stenoses by EBCT. Six of these segments (86%), but only 9 (29%) of the 31 correctly classified stenotic segments, were severely calcified (area >20 mm^2, p = 0.02). In 23 (12%) of 199 nonstenotic segments falsely classified as having ≥50% stenosis by EBCT, the lumen diameter was significantly smaller than that of the segments correctly classified as negative (mean [±SD] 1.5 ± 0.8 vs. 2.9 ± 1.1 mm, p < 0.001).**

Conclusions. **Intravenous EBCT coronary angiography allows for accurate segmental evaluation of significant disease in the major coronary arteries and may be of value for ruling out significant disease. The main determinant of false negative results is substantial segmental calcification, whereas the main determinant of false positive results is small vessel size.**

(J Am Coll Cardiol 1998;31:1547–54)

Direct visualization of the epicardial coronary arteries is necessary to establish the presence and focal severity of coronary lumen disease. At the moment, selective coronary angiography (SCA) is the only clinical method to accurately visualize and quantify coronary artery anatomy in vivo. Although this method provides for exceptional spatial resolution and a general "road map" of the coronary system, it is expensive, has a small but definite risk of complications and requires at least a brief hospital stay and a period of observation for several hours after the procedure (1). A convenient, noninvasive and safe means to perform coronary angiography clearly would be of clinical benefit.

Intravenous coronary angiography based on contrast-enhanced electron-beam computed tomography (EBCT) was introduced by Moshage et al. (2). Compared with other noninvasive approaches (3–6), EBCT offers a unique combination of superior temporal and spatial resolution with generation of a three-dimensional data set. Several published reports following the original report have confirmed the feasibility of using EBCT for the detection of stenoses in the coronary arteries (7–9) or venous and arterial bypass grafts (10). However, its potential for broad clinical applicability depends on 1) correct identification and localization of stenoses on a coronary segmental basis; and 2) exact definition of methodologic limitations related to variables such as vessel size, segmental anatomy and presence of coronary calcification. The purpose of this study was to evaluate these issues in patients undergoing SCA for the traditional assessment of coronary artery disease.

From the Division of Cardiovascular Diseases, Department of Internal Medicine and Department of Diagnostic Radiology, Mayo Clinic and Foundation, Rochester, Minnesota; and †Thorax Center, Rotterdam, The Netherlands. This study was funded by the Mayo Foundation (Grant 342-X-96), which also partly supported Dr. Rumberger. Dr. Schmermund was supported by a grant from the German Research Association (Deutsche Forschungsgemeinschaft, Schm 1233/1-1, Bonn) and a Heart Center Essen Cardiovascular Research Grant (Schm 97-1). Dr. Rensing was supported by a grant from the Dutch Interuniversity Cardiology Institute (ICIN), Utrecht, The Netherlands.

Manuscript received August 29, 1997; revised manuscript received November 25, 1997, accepted February 25, 1998.

*Present address and address for correspondence: Dr. Axel Schmermund, Department of Cardiology, University Clinic Essen, Hufelandstrasse 55, D-45122 Essen, Germany. E-mail: tka0i0@sp2.power.uni-essen.de.

Published by Elsevier Science Inc.

0735-1097/98/$19.00
PII S0735-1097(98)00132-6

Abbreviations and Acronyms

CI = confidence interval
EBCT = electron-beam computed tomography (tomographic)
ECG = electrocardiogram, electrocardiographic
LAD = left anterior descending coronary artery
LCx = left circumflex coronary artery
QCA = quantitative coronary angiography
RCA = right coronary artery
SCA = selective coronary angiography

Methods

Patients. The study was approved by the Mayo Clinic Institutional Review Board, and all patients provided written informed consent before participation. Thirty patients undergoing diagnostic SCA agreed to participate and to have EBCT performed within 24 h of SCA. Owing to technical problems with the image storage medium (an optical disk), data on two patients were irretrievable, and therefore we report the results from 28 consecutive patients. The patients' mean (±SD) age was 60 ± 11 years (range 39 to 75); there were 19 men and 9 women. Their mean body mass index was 26.5 ± 3.6 kg/m^2 (range 17.9 to 38.0). Eleven patients had a previous myocardial infarction, and 18 were taking beta-blockers.

Selective coronary angiography. SCA (Judkins technique) was performed with a minimum of five views of the left system and two views of the right system. All patients received 0.4 mg of nitroglycerin sublingually before imaging. The angiograms were visually assessed by two experienced angiographers who had no knowledge of the results of EBCT. Segmental stenoses estimated to represent ≥50% lumen diameter reduction were judged to be "significant." Quantitative coronary angiography (QCA), using a system validated in our laboratory (11), was performed to confirm these visual estimations and to determine a more precise degree of stenosis in the projection judged to show the worst narrowing. To assess the potential contribution of lumen size to the accuracy of the EBCT evaluation, the length of the lesion with an absolute lumen diameter ≤1.5 mm was computed for all significant stenoses determined by QCA, except in cases of total vessel occlusion. This diameter was chosen because the effective slice thickness using our protocol was 1 mm. Vessels with dimensions on this order thus had a potential for limited resolution, especially if not lying perpendicular to the tomographic imaging plane.

Twelve distinct coronary segments, as defined by the American Heart Association (12) (Fig. 1), were used for the SCA analysis and for comparison with intravenous EBCT coronary angiography. All segments were scored depending on the presence and severity of stenoses: 1 = angiographically normal segment (0% stenosis); 2 = nonobstructive disease (>0% to 49% lumen diameter stenosis); 3 = 50% to 74% lumen diameter stenosis; 4 = 75% to 99% lumen diameter stenosis; and 5 = total occlusion (100% lumen diameter stenosis). In segments visually estimated to contain significant stenoses (on the order of ≥50% diameter narrowing), the final classification of segments in categories 2 through 4 was based on QCA measurements. Finally, the minimal and reference lumen diameters of all coronary segments, irrespective of the presence of stenoses, were determined by QCA.

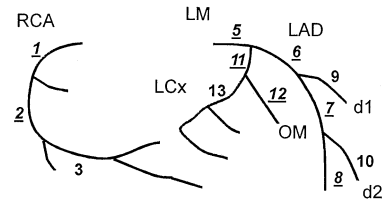

Figure 1. Segmental classification of the coronary artery tree as suggested by the American Heart Association (12). The **numbers not underlined** indicate the 12-segment model (major coronary arteries and side branches), and the **underlined numbers** indicate the eight-segment model (proximal major coronary arteries without side branches). d1 = first diagonal branch of LAD; d2 = second diagonal branch of LAD; LM = left main coronary artery; OM = first obtuse marginal branch of LCx.

In three patients, three coronary segments were distal to an occluded segment not supplied by collateral vessels and were excluded from the analysis. In three more patients, one lesion per patient was treated by balloon angioplasty before the EBCT examination. These segments were also excluded from the analysis because of the potential for factors such as early postprocedural restenosis or arterial spasm, which might confound comparison with EBCT.

Electron-beam computed tomography. A Siemens Evolution EBCT scanner (Imatron C-150LXP) was used. A routine examination of coronary calcium without contrast enhancement was obtained in all patients using a standardized protocol (13,14). Quantifiable segmental calcium was evaluated as reported by Baumgart et al. (15) and, slightly modified, by Kajinami et al. (16). A total calcium score was computed as the sum of all segmental scores (13,14).

For the intravenous EBCT coronary angiogram, images were obtained in 100 ms after an electrocardiographic (ECG) trigger signal at 80% of the RR interval. A tomographic slice thickness of 3 mm and a patient table increment of 2 mm, as suggested by Moshage et al. (2), resulted in overlapping slices with a nominal thickness of 1 mm. Imaging was done using an 18- or 21-cm field of view depending on individual heart size. A matrix size of 512 × 512 pixels yielded in-plane pixel dimensions of 0.35 × 0.35 mm (18-cm field of view) or 0.41 × 0.41 mm (21-cm field of view). Tomographic imaging commenced at the level of the aortic root above the coronary ostia. Patients were instructed to briefly hyperventilate just before scanning and then to hold their breath for the duration of the examination. A nonionic, reduced osmolar contrast medium (iopamidol 370) was injected through an 18-gauge angiocath into an antecubital vein with the use of a powered injector. The circulation time was determined by a 10-ml bolus of contrast medium and measurements of computed tomographic (CT) density values over 10 preset time frames over roughly 20 s in

the ascending aorta. For the intravenous coronary angiogram, the contrast agent was injected at a rate of 4 ml/s, and imaging commenced at the "circulation time" plus 3 s. The total volume of contrast agent injected ranged from 120 to 160 ml. It depended on the patient's heart rate and the time needed for continuous opacification of the coronary artery lumen. Forty "slices" scanned one at a time with each cardiac cycle required 40 s at a heart rate of 60 beats/min and 20 s at a heart rate of 120 beats/min. To cover a time of 40 s, 160 ml had to be given (4 ml/s), and to cover 20 s, 80 ml had to be given. To ensure adequate opacification, we gave a minimum of 110 ml per patient for the EBCT coronary angiogram in this initial series, but we did not give >150 ml. This added up to 120 to 160 ml, including the 10 ml of contrast agent used for determining circulation time.

The first five patients entered into the study were scanned in the neutral (transaxial) position. Interim analysis of images showed that artifacts obscuring the tomographic trajectory of the mid right coronary artery (RCA) could be decreased by tilting the patient table up by 10° and slewing it to the patient's right by 10°; this position was used for all subsequent examinations. The initial software configuration of the scanner limited the examination of most patients to 40 tomographic slices (covering ~8 cm); however, a software update available for examination of the last five patients enabled up to 120 slices, so that 50 to 60 slices through the entire cardiac volume could be obtained (covering ~10 to 12 cm).

The mean heart rate at baseline was 69 ± 10 beats/min (range 55 to 100). Because the EBCT allowed ECG-triggered scanning at each cardiac cycle up to heart rates of 120 beats/min, and because with higher heart rates the breathholding time is shorter due to the increased scanning frequence, it was our aim to examine patients with heart rates ≥80 beats/min. We thus administered 0.4 to 1.0 mg of intravenous atropine to 23 patients with rest heart rates <75/min. Sublingual nitroglycerin (0.4 mg) was administered to 21 patients for dilation of the coronary epicardial arteries. Seven patients refused to take nitroglycerin or had a headache at the time of the EBCT study. During EBCT coronary angiography, the mean heart rate increased to 81 ± 13 beats/min (range 60 to 110, $p < 0.001$ vs. baseline heart rate using the paired *t* test). No side effects were noted with the use of atropine and nitroglycerin, except for oral dryness in several patients. Total breathholding time was 34 ± 5 s (range 25 to 42) and was well tolerated by all patients.

All two-dimensional tomograms were evaluated for image quality, patient motion, correct ECG triggering, arterial contrast opacification and presence of extensive focal calcium deposits. The EBCT-derived three-dimensional angiographic data were processed on a Siemens Magic View workstation according to the suggestions by Moshage et al. (2) and Achenbach et al. (7,10). This workstation allows rendering of three-dimensional volumetric images from the overlapping two-dimensional tomograms and was used to analyze the images in several different ways. For three-dimensional rendering analysis, the tomographic frames were manually edited so as to include all contrast-enhanced cardiac structures and to provide for an overview of the heart as a whole. Portions of the left and right atria were excluded on an individual basis to allow for better assessment of the proximal left circumflex coronary artery (LCx) and RCA, respectively. As a first step, these data were rendered as a "shaded surface display" (i.e., display of gray scale [density] values of the leading edge of each structure within a preset range of density values) (Fig. 2a). According to the method of Achenbach et al. (7), an EBCT density of 80 Hounsfield units was chosen as the lower threshold so as to exclude nonenhanced cardiac structures; however, no upper threshold density limit was set. In a second step, only the aortic root and coronary epicardial arteries were edited to be included in the three-dimensional representation. This data set was rendered as "shaded surface display" as described earlier (Fig. 2b), and also as "maximal intensity projection". In this latter projection, only the maximal density values at each point in the three-dimensional volume are displayed, and the final picture is similar to a conventional (arterial) angiogram in that structures are projected over one another. In addition, "curved surface reformation" (also termed "multiplanar reformation") was obtained of the major coronary arteries in all patients. In this technique, the plane of a specific artery is chosen to be displayed as a two-dimensional image. This then represents a "curved surface" from within the three-dimensional volume, following the curved trajectory of the respective artery (Fig. 2d). The final interpretation of any individual EBCT coronary angiogram was based on an integrated opinion based on all image rendering techniques.

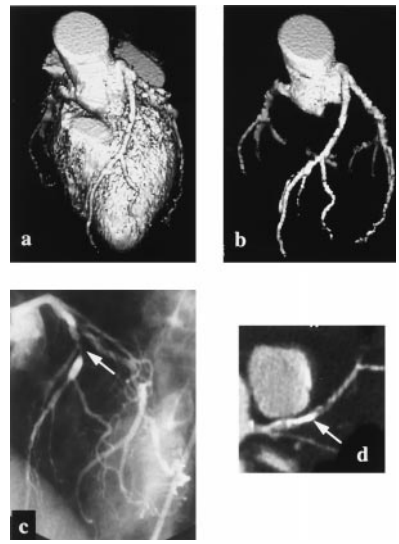

Figure 2. Comparison of intravenous EBCT coronary angiography and SCA in a 69-year old woman. **a,** EBCT: shaded surface rendering of the whole heart. The left coronary system appears normal. **b,** EBCT: shaded surface rendering of the coronary arteries. The left coronary system appears normal. **c,** SCA: 55% lumen diameter stenosis in the proximal LAD (segment 6, **arrow**) is evident, which was not visualized by EBCT. **d,** EBCT: curved surface rendering (multiplanar reformation) of the LAD. Extensive calcification in the proximal LAD (segment 6, **arrow**) creates high EBCT density values that can be mistaken to represent contrast opacification in the shaded surface display. This may explain the false negative result.

Table 1. Comparison Between Intravenous Electron-Beam Coronary Angiography and Selective Coronary Angiography in 330 Segments Comprising the Major Coronary Arteries and Side Branches in 28 Patients

EBCT Segmental Classification	SCA Segmental Classification					
	1	2	3	4	5	Total
1	**87**	50	4	2	0	143
2	10	**29**	1	0	0	40
3	4	7	**13**	2	0	26
4	3	5	6	**2**	1	17
5	2	2	2	1	**4**	11
Nonassessable	68	19	2	4	0	93
Total	174	112	28	11	5	330

$p < 0.001$, chi-square 170.0, contingency coefficient 0.65. EBCT = electron-beam computed tomography; SCA = selective coronary angiography. Classification of segments: 1 = normal segment as judged by SCA/EBCT; 2 = nonobstructive disease (i.e., >0% to 49% lumen diameter stenosis); 3 = 50% to 74% lumen diameter stenosis; 4 = 75% to 99% lumen diameter stenosis; 5 = total occlusion. Numbers in boldface indicate exact agreement between both techniques.

The EBCT coronary angiographic three-dimensional images were analyzed on the same segmental basis as the SCAs (12), defined with reference to angiographic anatomic landmarks such as vessel bifurcations and side branches, which could readily be identified from the EBCT coronary angiograms. Analysis was performed in the 12 angiographically defined segments representing the major coronary arteries and side branches (Fig. 1) to duplicate the analysis of the SCA. In a separate analysis that excluded side branches, only eight segments in the proximal major coronary arteries were considered. The EBCT coronary angiograms were evaluated by two investigators who had no knowledge of the results of SCA and who reached agreement on their classification replicating the grading system (1 through 5) used for the selective angiograms. Interobserver variability for EBCT was tested in nine randomly selected patients in whom a second team of two investigators analyzed the coronary segments, without knowledge of either the SCA or the initial EBCT readings.

Statistics. Statistical analyses were performed using SPSS (version 6.1.4), MedCalc (4.16) and a desktop computer. Data are reported as the mean value ± SD, unless otherwise indicated. The segmental classification of the SCA and the presence of significant stenoses determined by QCA were considered the "true" observations against which segmental EBCT variables were compared. The standard errors for sensitivity, specificity, positive and negative predictive values and accuracy were determined as described by Diamond and Forrester (17). Characteristics of groups of patients or coronary segments were compared using an unpaired or paired *t* test where appropriate. Proportions were compared by the chi-square test. Kappa statistics were used to evaluate interobserver agreement. To test for independence of the results for different segments in the same patients, chi-square analysis of independence was performed. Also, the correlation between intraperson mean segmental gradings from SCA and those from EBCT was tested for homogeneity across patients. A p value <0.05 was considered significant for all statistical evaluations.

Results

Selective coronary angiography. Of the 28 patients, 18 (64%) had at least one significant stenosis (50% to 100% lumen diameter stenosis, grades 3 to 5), 8 (29%) had nonobstructive disease (no segments graded >2) and 2 (7%) had angiographically normal coronary arteries (only segments graded 1). In the 18 patients with significant angiographic disease, a total of 47 significant segmental stenoses (graded ≥3) were noted: 22 in the left anterior descending coronary artery (LAD), 11 in the LCx and 14 in the RCA. Ten patients had one-vessel disease, two had two-vessel disease and six had three-vessel disease. There were no significant stenoses of any left main coronary artery segment.

Of the 47 segments graded ≥3, 44 (94%) were located in the major coronary arteries or major side branches for the 12-segment model. Thirty-seven segments graded ≥3 (79%) were seen in the proximal major coronary arteries without side branches for the eight-segment model. Of note, no patient had a segmental stenosis ≥50% outside the eight-segment model (either in the 12-segment model or further distal) who did not also have a proximal stenosis ≥50%.

Electron-beam computed tomography. Quantifiable coronary calcium was found in 25 patients (89%). No calcium was seen in three patients: two with angiographically normal coronary arteries and one with nonobstructive disease who had six segments graded 2. The mean total calcium score was higher in patients with obstructive angiographic disease (segments graded ≥3, n = 18) than in patients with nonobstructive angiographic disease (segments graded 2, n = 8) (996.7 ± 775.1 [range 18.5 to 2366.9] vs. 179.4 ± 230.5 [range 0 to 583.3], $p = 0.001$).

Of the 330 coronary segments assessable from SCA (12 segments per patient with six segments excluded from the analysis), 237 (72%) were visualized by EBCT. Table 1 gives an overview of the comparison between EBCT and SCA with respect to the coronary segmental disease grade. Table 2 provides the same data using the eight-segment model. In this

Table 2. Comparison Between Intravenous Electron-Beam Coronary Angiography and Selective Coronary Angiography in 221 Segments Comprising the Proximal and Mid Major Coronary Arteries (eight-segment model) in 28 Patients

EBTC Segmental Classification	SCA Segmental Classification					
	1	2	3	4	5	Total
1	**70**	44	3	2	0	119
2	7	**24**	1	0	0	32
3	3	5	**13**	1	0	22
4	2	2	5	**2**	1	12
5	1	1	0	3	**4**	9
Nonassessable	19	7	1	0	0	27
Total	102	83	23	8	5	221

$p < 0.0001$, chi-square 192.8, contingency coefficient 0.71. Abbreviations, symbols and classification of segments as in Table 1.

case, three segments were excluded owing to balloon angioplasty at the time of SCA. Of the 221 remaining segments, 194 (88%) were visualized by EBCT. Nonobstructive angiographic disease (segments graded 2) were frequently underestimated from EBCT, whereas obstructive disease (segments graded 3) were most often correctly classified or even overestimated from EBCT. The contingency coefficient as a measure of the degree of the relation between SCA and EBCT was 0.65 for the 12-segment model and 0.71 for the 18-segment model (chi-square statistics; 1 being the optimal value). There was a significant correlation between intraperson mean segmental grading from SCA and that from EBCT ($R^2 = 0.5$, $p = 0.0065$), indicating that the segmental comparisons described earlier were homogeneous across patients and not due to "clusters" in some of the patients.

Table 3 gives sensitivity and specificity data with regard to the diagnosis of significant stenoses by EBCT (grades 3 to 5 vs. 1 or 2) for analysis of either 12 or 8 segments per patient and compares the overall results with those obtained for each of the major coronary arteries. Consistently, the negative predictive values were high (93% to 100%) and better than the positive predictive values (25% to 84%), and a better overall accuracy was achieved in the LAD than in the RCA or LCx. There was no significant heterogeneity across patients, as the chi-square analysis of independence yielded p values of 0.7 for sensitivity and 0.16 for specificity across patients. In other words, the distribution of sensitivities and specificities was not different from a random distribution in our patients.

Table 4 gives the results yielded by two independent groups of observers in nine randomly selected patients. Although some variability was noted with regard to classification of segments graded 1 or 2, only one lesion was scored "significant" by one group of observers and "nonsignificant" by the other group. This was in an ostial lesion with a 59% diameter stenosis of the first obtuse marginal branch in a patient in whom two LAD lesions were correctly identified by both groups of observers. However, a total of four stenoses were described by one group of observers and judged "nonassessable" by the other group. The mean (±SE) kappa statistic was 0.88 ± 0.04 (95% confidence interval [CI] 0.80 to 0.97) if calculated with respect to the segmental differentiation of significant angiographic stenoses from minor or no disease, including judgment of segment assessability, and it was 0.59 ± 0.06 (95% CI 0.46 to 0.71) for the overall grading.

A total of seven significant stenoses (18% of 38 segments graded ≥3 by coronary angiography) were not detected by EBCT (Table 1, Fig. 2): three in the LAD, three in the LCx and one in the RCA. These lesions tended to have a less severe diameter stenosis, a larger minimal lumen diameter and a shorter segment measuring ≤1.5 mm in absolute diameter than lesions that were detected by EBCT, but these differences were not statistically significant (Table 5). However, the area of

Table 3. Sensitivity and Specificity Data for the Detection of Angiographically Significant Stenoses (≥50% diameter stenosis) With Electron-Beam Computed Tomography

	12-Segment Model					8-Segment Model				
	Total (n = 237)	LMCA (n = 28)	LAD (n = 89)	LCx (n = 54)	RCA (n = 66)	Total (n = 194)	LMCA (n = 28)	LAD (n = 75)	LCx (n = 40)	RCA (n = 51)
Sensitivity	82 ± 6	—	84 ± 8	50 ± 19	91 ± 9	83 ± 6	—	82 ± 9	75 ± 22	90 ± 9
Specificity	88 ± 2	100 ± 0	96 ± 2	80 ± 6	81 ± 5	91 ± 2	100 ± 0	98 ± 2	81 ± 7	83 ± 6
PPV	57 ± 7	—	84 ± 8	25 ± 13	50 ± 12	67 ± 7	—	93 ± 7	30 ± 15	59 ± 12
NPV	96 ± 2	100 ± 0	96 ± 2	93 ± 4	98 ± 2	96 ± 2	100 ± 0	93 ± 3	97 ± 3	97 ± 3
Accuracy	87 ± 2	100 ± 0	93 ± 3	77 ± 6	83 ± 5	90 ± 2	100 ± 0	93 ± 3	80 ± 6	84 ± 5

Data for all segments and for the major coronary arteries given separately. LAD = left anterior descending coronary artery; LCx = left circumflex coronary artery; LMCA = left main coronary artery; NPV = negative predictive value; PPV = positive predictive value; RCA = right coronary artery.

Table 4. Analysis of Coronary Segments (12 per patient) by Intravenous Electron-Beam Computed Tomographic Coronary Angiography

Investigator Group 2 Segmental Classification	Investigator Group 1 Segmental Classification						
	1	2	3	4	5	Nonassessable	Total
1	**40**	8	0	0	0	0	48
2	8	**6**	1	0	0	1	16
3	0	0	**4**	5	0	1	10
4	0	0	2	**1**	1	0	4
5	0	0	0	0	**1**	0	1
Nonassessable	0	1	0	1	2	23	27
Total	48	15	7	7	4	25	106

Evaluation was done by two teams of independent investigators in nine randomly selected patients. Symbols and classification of segments as in Table 1.

calcium attributed to the stenotic segments was significantly greater in stenoses not detected by EBCT than that in stenoses that were detected, and the segmental calcium scores were also significantly higher (Table 5, Fig. 2 and 3). In 6 (86%) of the 7 stenoses not detected by EBCT, calcific lesions of an area >20 mm^2 were found, although this degree of segmental calcification was seen in only 9 (29%) of the 31 stenoses correctly identified by EBCT ($p = 0.02$, chi-square and Fisher exact tests).

A total of 23 (12%) of 199 segments graded 1 or 2 by SCA were misdiagnosed as showing ≥50% diameter stenosis by EBCT (Table 1, Fig. 4). These falsely positive segments had a significantly smaller lumen caliber than the truly negative segments (Table 5).

A total of 93 segments were not visualized adequately to be judged assessable by EBCT (Table 1). These comprised segments including the first two diagonal branches of the LAD (n = 41) or the distal LCx (n = 15) (i.e., segments significantly smaller than the remaining major epicardial segments). Reference vessel size and minimal lumen diameter were 1.9 ± 0.7 mm and 1.4 ± 0.5 mm, respectively, for nonassessable segments, compared with 2.6 ± 1.2 mm and 2.1 ± 1.2 mm, respectively, for assessable segments ($p < 0.001$ for both comparisons between nonassessable and assessable segments). Other factors accounting for nonaccessibility by EBCT included localization of segments distal to severe stenoses (n = 15), presence of severe diffuse disease and subtotal occlusion (n = 4) or hypoplastic vessels with reference diameters <1 mm (n = 15). Only one segment could not be assessed owing to a premature supraventricular contraction and improper ECG triggering.

On a patient-by-patient basis, 21 (75%) of the 28 patients were correctly classified with respect to significant coronary artery disease by EBCT (true positive or true negative results; 16 men and 5 women), 2 (7%) had false negative results (1 man and 1 woman) and 5 (18%) had false positive results (2 men and 3 women). Both patients with false negative results had LAD stenoses of borderline angiographic significance (50% and 55% diameter stenosis by QCA) and were not thought to require catheter or surgical interventions by the attending clinicians. Their individual EBCT total calcium scores were 429.11 and 1,244.72, and thus, on the basis of total atherosclerotic plaque burden alone, the presence of significant coronary artery disease was suspected (18). In contrast, calcium scores were significantly higher in patients with true positive than in those with false positive results (Fig. 5). The number of segments not assessable by EBCT per patient did not differ between those correctly or incorrectly classified (3.7 ± 1.1 vs. 3.3 ± 2.2, $p = 0.7$).

Table 5. Angiographic Characteristics and Segmental Calcification of Segments With False Negative Results (n = 7) Versus True Positive Results (n = 31) and Angiographic Characteristics of Segments With True Negative Results (n = 199) Versus False Positive Results (n = 23) by Electron-Beam Computed Tomography

	False Negative Results		False Positive Results	
	EBCT FN	EBCT TP	EBCT FP	EBCT TN
Diameter stenosis (%)	64.0 ± 9.9	72.4 ± 18.2	14.9 ± 13.8	17.3 ± 12.0
Length of segment ≤1.5 mm (mm)	3.8 ± 2.9	4.9 ± 3.3	—	—
Minimal lumen diameter (mm)	0.91 ± 0.34	0.84 ± 0.29	1.2 ± 0.6	2.3 ± 1.1†
Reference diameter (mm)	2.55 ± 0.43	2.44 ± 0.52	1.5 ± 0.8	2.9 ± 1.1†
Area of calcification (mm^2)	39.5 ± 15.9	21.2 ± 24.1*	—	—
Segmental calcium score	157.4 ± 64.3	83.0 ± 97.3*	—	—

*$p < 0.05$ versus false negative (FN). †$p < 0.001$ versus false positive (FP). EBCT = electron-beam computed tomographic; TN = true negative; TP = true positive.

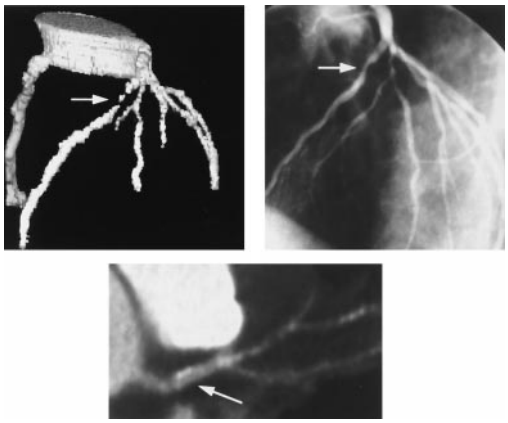

Figure 3. Comparison of intravenous EBCT coronary angiography and SCA in a 49-year old man. The **left upper panel** shows an EBCT shaded surface display with correct detection of a proximal 68% lumen diameter stenosis of the LAD (selective angiogram, **right**). The stenosis was overestimated and graded as 4 from EBCT as opposed to 3 from SCA. The **lower panel** shows a curved surface rendering (multiplanar reformation) of the LAD with comparably little calcification. The **arrows** indicate the site of the lesion.

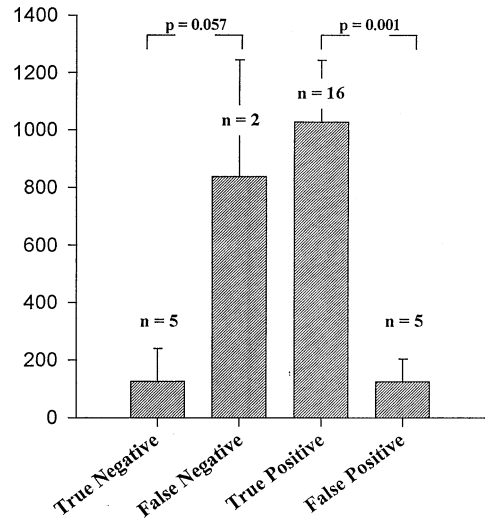

Figure 5. Total coronary calcium scores (mean ± SE) as a function of classification of patients from intravenous EBCT coronary angiography. Patients with false positive results had calcium scores similar to those with true negative results, and patients with false negative results had calcium scores similar to those with true positive results.

Discussion

This investigation evaluated the application of intravenous EBCT for a minimally invasive definition of major coronary artery anatomy on a segmental basis and, to our knowledge, represents the first attempt to characterize limitations of the technique. No patients with available images were excluded from the analysis. Concordant with previous reports (2,9,19), good sensitivity and a very high negative predictive value for ruling out obstructive coronary lumen disease were found. However, positive predictive accuracy was only moderate. Marked segmental coronary calcium was determined to be the most important factor related to false negative interpretation of lumen disease severity. Of 7 "false negative" lesions, 6 (86%) showed a segmental calcium area >20 mm^2. Kaufmann et al. (20), using receiver operating characteristic curve analysis in 160 patients, found that a calcium area of 18 mm^2 best separated individuals with from those without obstructive lumen disease, and accordingly the presence of severe segmental calcification would alert the clinician to the high likelihood of obstructive coronary artery disease. A larger reference lumen diameter and a shorter stenosis segment (≤1.5 mm) may also have played a role in cases where stenosis severity was underestimated, but to a much lesser degree than segmental coronary calcium (Table 5). Small vessel diameter was the main determinant of falsely positive results. Small vessel diameter was also associated with segments judged to be nonassessable, along with factors such as upstream high grade stenoses or severe diffuse disease of the segment in question. Artifacts caused by improper ECG triggering or patient movement and breathing were rare and did not have a major impact on the results.

Figure 4. Comparison of intravenous EBCT coronary angiography and SCA in a 41-year old man without angiographically significant stenoses. From EBCT (**left),** a significant stenosis of the first diagonal branch of the LAD was incorrectly diagnosed (**arrow**). SCA (**right**) shows that this diagonal branch had a small reference lumen diameter (1.91 mm, **arrow**), a factor that may have contributed to the false positive result from EBCT.

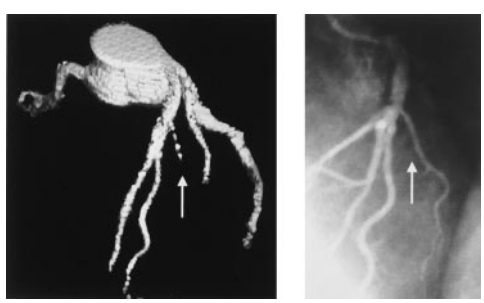

Factors contributing to technical limitations of EBCT. We classified 93% of all LAD segments correctly, but accuracy declined to 83% to 84% for RCA segments and to 77% to 80% for LCx segments. This difference in accuracy for the major coronary arteries is very comparable to previously reported results (2,9,19). Although other investigators (2) have suspected motion artifacts as the explanation, more apparent in the LCx and RCA than in the LAD, a smaller vessel diameter was the most important factor confounding the grading of LCx segments in our study. For RCA segments, several factors may have been contributing. Despite modification of patient positioning in the last 23 of 28 EBCT studies, persistent artifacts in the mid-RCA were seen due to the dense contrast opacification of the adjacent right atrium. Also, as opposed to angiographically normal coronary arteries in a larger group of patients undergoing SCA (21), major RCA segments (n = 51) in our patients had a significantly smaller reference lumen

diameter than major LAD segments (n = 75) (2.5 ± 1.1 vs. 3.1 ± 0.9 mm, p = 0.004).

EBCT image analysis. Because the interpretation of shaded surface three-dimensional rendering relies on gray scale (density) values above the preset threshold, it has been previously speculated that calcium may be difficult to differentiate from contrast opacification owing to the overlap in density values (2). Multiplanar reformation instead of a shaded surface display has been suggested as a means to circumvent this shortcoming (8). With this approach, however, uncertainties as to the true center of the vessel may be of concern. Maximal intensity projections have been used to detect calcium (2), but they may not always permit reliable detection of stenoses because of the overlap of different structures in the planar projection format. Realizing from the outset that no single method of analysis is without limitations, we incorporated review of the two-dimensional images, including the calcium scans, and the different three-dimensional renderings into our final consensus opinions.

Conclusions. Intravenous EBCT coronary angiography is an attractive method for the noninvasive definition of coronary anatomy because it can be performed in a straightforward fashion, requires an examination time of only minutes, is associated with a very steep learning curve and provides highly reproducible results (2,8,9,19). Our study confirms high negative predictive values with respect to the detection and localization of obstructive stenoses on a segmental basis. This suggests that EBCT coronary angiography may be of value for ruling out significant disease in patients undergoing clinical evaluation for obstructive versus nonobstructive coronary artery disease. Therefore, it should be analyzed in the context of the patient's history and symptoms. Calcium quantities, as a surrogate measure for intramural atherosclerotic plaque burden, may be especially valuable in cases with equivocal findings related to diffuse coronary disease and a small vessel lumen diameter (14,18).

We thank Dr. John F. Bresnahan for his valuable help in grading the selective coronary angiograms; Dr. Suvipaporn Siripornpitak for her valuable help in grading the EBCT angiograms; and Joseph F. Colter for his expert assistance in performing quantitative angiographic analyses.

References

1. Pepine CJ, Allen HD, Bashore TM, et al., American College of Cardiology/American Heart Association Ad Hoc Task Force on Cardiac Catheterization. ACC/AHA guidelines for cardiac catheterization and cardiac catheterization laboratories. Circulation 1991;84:2213–47.
2. Moshage WE, Achenbach S, Seese B, Bachmann K, Kirchgeorg M. Coronary artery stenoses: three-dimensional imaging with electrocardiographically triggered, contrast agent-enhanced, electron-beam CT. Radiology 1995;196:707–14.
3. Hamm CW, Meinertz T, Dix WR, et al. Intravenous coronary angiography with dichromography using synchrotron radiation. Herz 1996;21:127–31.
4. Manning WJ, Li W, Edelman RR. A preliminary report comparing magnetic resonance coronary angiography with conventional angiography [erratum in N Engl J Med 1994;330:152]. New Engl J Med 1993;328:828–32.
5. Pennell DJ, Bogren HG, Keegan J, Firmin DN, Underwood SR. Assessment of coronary artery stenosis by magnetic resonance imaging. Heart 1996;75:127–33.
6. Caiati C, Aragona P, Iliceto S, Rizzon P. Improved Doppler detection of proximal left anterior descending coronary artery stenosis after intravenous injection of a lung-crossing contrast agent: a transesophageal Doppler echocardiographic study. J Am Coll Cardiol 1996;27:1413–21.
7. Achenbach S, Moshage W, Ropers D, Nossen J, Bachmann K. Nichtinvasive Koronarangiographie mittels Elektronenstrahltomogaphie: Methodik und klinische Evaluierung im Follow-up nach PTCA. Z Kardiol 1997;86:121–30.
8. Nakanishi T, Ito K, Imazu M, Yamakido M. Evaluation of coronary artery stenoses using electron-beam CT and multiplanar reformation. J Comput Assist Tomogr 1997;21:121–7.
9. Budoff MJ, Oudiz RJ, Zalace CP, et al. Intravenous three dimensional coronary angiography using contrast enhanced electron beam computed tomography [abstract]. J Am Coll Cardiol 1997;29 Suppl A:393A.
10. Achenbach S, Moshage W, Ropers D, Nossen J, Bachmann K. Noninvasive, three-dimensional visualization of coronary artery bypass grafts by electron beam tomography. Am J Cardiol 1997;79:856–61.
11. Bell MR, Britson PJ, Chu A, Holmes DR Jr, Bresnahan JF, Schwartz RS. Validation of a new UNIX-based quantitative coronary angiographic system for the measurement of coronary artery lesions. Cathet Cardiovasc Diagn 1997;40:66–74.
12. American Heart Association Committee Report. A reporting system on patients evaluated for coronary artery disease. Circulation 1975;51:7–34.
13. Agatston AS, Janowitz WR, Hildner FJ, Zusmer NR, Viamonte M, Detrano R. Quantification of coronary artery calcification using ultrafast CT. J Am Coll Cardiol 1990;15:827–32.
14. Rumberger JA, Sheedy PF, Breen JR, Schwartz RS. Coronary calcium as determined by electron beam CT, and coronary disease on arteriogram: effect of patient's sex on diagnosis. Circulation 1995;91:1363–7.
15. Baumgart D, Schmermund A, Görge G, et al. Comparison of electron beam computed tomography with intracoronary ultrasound and coronary angiography for the detection of coronary atherosclerosis. J Am Coll Cardiol 1997;30:57–64.
16. Kajinami K, Seki H, Takekoshi N, Mabuchi H. Coronary calcification and coronary atherosclerosis: site by site comparative morphologic study of electron beam computed tomography and coronary angiography. J Am Coll Cardiol 1997;29:1549–56.
17. Diamond GA, Forrester JS. Analysis of probability as an aid in the clinical diagnosis of coronary-artery disease. N Engl J Med 1979;300:1350–8.
18. Rumberger JA, Sheedy PF, Breen JF, Schwartz RS. Electron beam computed tomographic calcium score cutpoints and severity of associated angiographic lumen stenosis. J Am Coll Cardiol 1997;29:1542–8.
19. Achenbach S, Moshage W, Nossen J, et al. Nichtinvasive Koronararteriendarstellung mittels Elektronenstrahltomographie—Vergleich zur Koronarangiographie bei 100 Patienten [abstract]. Z Kardiol 1997;86 Suppl 2:205.
20. Kaufmann RB, Moll PP, Sheedy PF, Rumberger JA, Schwartz RS. Quantification of coronary artery calcium by electron beam computed tomography for determination of angiographic coronary artery disease in younger individuals. J Am Coll Cardiol 1995;25:626–32.
21. Dodge JT Jr, Brown BG, Bolson EL, Dodge HT. Lumen diameter of normal human coronary arteries—influence of age, sex, anatomic variation, and left ventricular hypertrophy or dilation. Circulation 1992;86:232–46.